

Regularized autoregressive modeling and its application to audio signal declipping

Ondřej Mokřý, Pavel Rajmic

Abstract—Autoregressive (AR) modeling is invaluable in signal processing, in particular in speech and audio fields. Attempts in the literature can be found that regularize or constrain either the time-domain signal values or the AR coefficients, which is done for various reasons, including the incorporation of prior information or numerical stabilization. Although these attempts are appealing, an encompassing and generic modeling framework is still missing. We propose such a framework and the related optimization problem and algorithm. We discuss the computational demands of the algorithm and explore the effects of various improvements on its convergence speed. In the experimental part, we demonstrate the usefulness of our approach on the audio declipping problem. We compare its performance against the state-of-the-art methods and demonstrate the competitiveness of the proposed method, especially for mildly clipped signals. The evaluation is extended by considering a heuristic algorithm of generalized linear prediction (GLP), a strong competitor which has only been presented as a patent and is new in the scientific community.

Index Terms—autoregression, regularization, inverse problems, audio declipping, proximal splitting methods, sparsity

I. INTRODUCTION

AUTOREGRESSIVE models have been used in a variety of engineering problems. Tasks currently solved with the help of autoregressive modeling include speech coding [1, Sec. 8.2.2], music analysis and coding [2, Ch. 4], and time series prediction in finance, for instance [3, Ch. 2]. AR processes have found their use also within the control theory [4], where a clear connection to Hankel operators exists [5], [6].

Fitting a signal with an autoregressive (AR) process possesses a kind of an inverse problem. Thus, where appropriate, it has found its use in reconstruction tasks where data are missing or where data are observed in a degraded form. In its simplest form, the AR fitting of a signal can be understood as a denoiser—the noise is identified with the residual error. A more complicated application example is the time series extrapolation or interpolation of missing segments of audio [7]. In some inverse problems, the prior knowledge about the signal can consist of more than only its AR nature. In such advanced cases, however, a need often arises to regularize or constrain the signal itself or even the AR coefficients. Common AR fitting algorithms are not suitable to cope with such augmented situations.

The contribution of this article is twofold. First, it presents general models which, beside common AR assumptions, allow

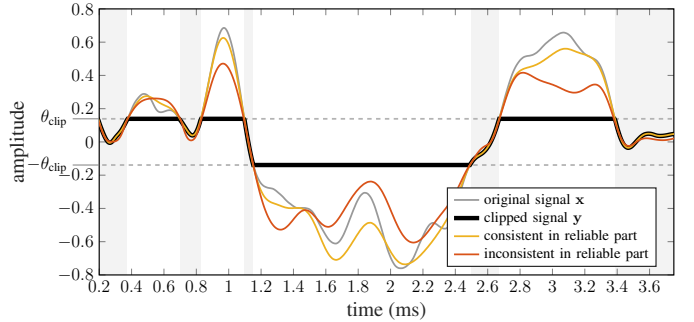


Fig. 1. Illustration of clipping and the consistency condition, adapted from [10].

additional regularization terms, and offers related numerical algorithms. Second, the theory is validated on an audio declipping problem; the proposed approach is moreover compared with the state of the art methods.

A. Audio declipping problem

Audio inpainting and audio declipping are two popular signal recovery tasks. In audio inpainting, signal samples are missing, and the inverse problem consists in reconstructing (i.e., estimating) them. Within an optimization framework, which is the most widely used recovery approach, this can be formulated as

$$\min_{\mathbf{x}} f(\mathbf{x}) \quad \text{s.t.} \quad \mathbf{x} \in \Gamma_{\text{inp}} = \{\mathbf{x} \in \mathbb{R}^N \mid M_{\text{R}}\mathbf{x} = M_{\text{R}}\mathbf{y}\}. \quad (1)$$

In this problem, a signal \mathbf{x} is sought such that it meets the requirements expressed by the penalization function f . At the same time, \mathbf{x} must perfectly fit the observed portion of the signal $\mathbf{y} \in \mathbb{R}^N$. Here, the masking operator M_{R} identifies the reliable samples in question. The condition $\mathbf{x} \in \Gamma_{\text{inp}}$ is often called the consistency condition [8].

In audio declipping, samples are not completely missing but, instead, are observed saturated (clipped), i.e., samples exceeding the dynamic range $[-\theta_{\text{clip}}, \theta_{\text{clip}}]$ are limited in amplitude according to the nonlinear formula [9], [10]

$$y_n = \begin{cases} x_n & \text{for } |x_n| < \theta_{\text{clip}}, \\ \theta_{\text{clip}} \cdot \text{sgn}(x_n) & \text{for } |x_n| \geq \theta_{\text{clip}}. \end{cases} \quad (2)$$

Here, \mathbf{x} is the input signal and \mathbf{y} is its observed counterpart, see an example in Fig. 1.

In such a case, the recovery problem reads

$$\min_{\mathbf{x}} f(\mathbf{x}) \quad \text{subject to} \quad \mathbf{x} \in \Gamma_{\text{declip}}, \quad (3)$$

O. Mokřý and P. Rajmic are with the SPLab at the Faculty of Electrical Engineering and Communication, Brno University of Technology, Czech Republic. E-mail: ondrej.mokry@vut.cz, pavel.rajmich@vut.cz,

where the consistency set Γ_{declip} corresponds to the element-wise clipping constraints $\pm\theta_{\text{clip}}$:

$$\Gamma_{\text{declip}} = \{\mathbf{x} \in \mathbb{R}^N \mid \begin{array}{l} M_R \mathbf{x} = M_R \mathbf{y} \\ M_H \mathbf{x} \geq \theta_{\text{clip}} \\ M_L \mathbf{x} \leq -\theta_{\text{clip}} \end{array} \}. \quad (4)$$

The respective masking operators M_R , M_H and M_L serve to pick samples from the corresponding set of indices $\{1, \dots, N\}$ [10].

In declipping, more information is available about the signal than in inpainting. Unfortunately, while the restriction $\mathbf{x} \in \Gamma_{\text{imp}}$ in (1) still allows solving it via the use of common AR fitting algorithms, the additional knowledge coded in $\mathbf{x} \in \Gamma_{\text{declip}}$ is not directly transferable into these algorithms, as will also be discussed in the following part.

B. Autoregressive methods for signal reconstruction

It is clear that any inpainting method can be used for declipping as well. This is achieved by simply ignoring the conditions involving M_H and M_L in (4). This is also the case of the Janssen method [11], [12] which is the state-of-the-art for audio inpainting for compact signal gaps of up to 80 ms in length [13], [14]. It is a blockwise, iterative approach where in each iteration, the AR coefficients are estimated for a whole block of a signal and then the missing samples are updated according to the model. In the next iteration, the model is re-estimated based on the current solution and the process is repeated in such a manner. Importantly, the iterations involve standard AR estimation only.

The patent [15] proposes a method for audio declipping, referred to as generalized linear prediction (GLP), that builds upon the idea of Janssen. The extension lies in that after each iteration, all samples currently violating the conditions $M_H \mathbf{x} \geq \theta_{\text{clip}}$, $M_L \mathbf{x} \leq -\theta_{\text{clip}}$ are flipped around the respective $\pm\theta_{\text{clip}}$ levels. This is quite a heuristic step but it surprisingly leads to an algorithm that is one of the best performing. The flipping operation on the signal, described by the authors as a rectification, forces the consistency in the clipped part. Interestingly, the method (the same as the patent) is practically ignored by the signal processing community. The algorithm of [15] represents one of the options how to cope with the clipping consistency, but it is purely heuristic. In our article, we will make an effort to formulate the constraints on the signal \mathbf{x} in a rigorous way and make it a part of the modeling task.

Other important AR-based methods for audio inpainting of compact gaps are those based on extrapolating the right- and left-hand sides of each gap separately; the interpolation task is then solved by crossfading the two extrapolated sequences [16]–[19]. Similarly, Etter [7] proposes to use separate AR models for the two contexts of the gap but suggests for the two sets of AR parameters to be optimized simultaneously. However, neither of these contributions involves any regularization or constraints and, most importantly, the extrapolation-based methods require long reliable context of the gap, which limits the use cases significantly.

An ARMA approach to modeling time series with sparsity constraints on both the AR and MA coefficients has been

presented in [20]. Later, the authors of [21], [22] presented their approach to audio inpainting under the name High-order sparse linear prediction (HOSpLP). The same as in the follow-up papers [23], [24], the goal is to recover missing samples of speech by using an AR model with sparsity regularization on the AR coefficients.

Importantly, none of the methods mentioned above offers a flexible interconnection between the AR model and the time-domain requirements on the signal.

The area of signal reconstruction has not been ignored by the advances in deep learning. In particular, declipping and inpainting has been treated by different deep models [25]–[28]. In the context of autoregression, two models should be mentioned: First, the popular WaveNet [29] has a conceptual connection with AR modeling, since the generation of signal samples is conditional, given the preceding samples. Second, the AR-Net [30] represents an equivalent description of the AR model, but from the perspective of neural networks. In particular, the AR coefficients are treated as network parameters and optimized using the back-propagation algorithm. This approach also allows to regularize the coefficients by simply adding terms to the loss function. As an example, the authors of [30] mention sparsity, creating a connection with the HOSpLP framework [21]. However, neither of the models offers to constrain the time-domain signal and direct applications to audio signal reconstruction is missing.

C. Our contribution

Inspired by the success of the heuristic GLP approach that can apply simple constraints in the time domain, and HOSpLP that regularizes the AR coefficients estimation with their sparsity, we propose a general framework that enables regularizing/constraining the time-domain and AR-domain estimation simultaneously. Our formulation stems from a theoretical foundation and leads to an optimization program, solvable with standard proximal algorithms.

The rest of the paper is organized as follows: An overview of the AR model and the notation is introduced in Sec. II, together with its regularized variant and with model fitting defined as an optimization task. An algorithm to solve the task is developed in Sec. III. Sec. IV demonstrates the suitability of the proposed method for the problem of audio declipping; we compare the performance of the discussed approaches with that of other optimization-based methods. Effects of different parameters of the proposed model and of the algorithm are also presented. Finally, Sec. V concludes the paper. Appendix A is devoted to considerations on acceleration of the numerical solver. Appendix B provides implementation details.

II. AUGMENTING THE AUTOREGRESSIVE MODEL

An autoregressive process of the order p is a discrete-time stochastic process $\{X_n \mid n = 0, \pm 1, \pm 2, \dots\}$ defined by the equation

$$X_n + a_2 X_{n-1} + \dots + a_{p+1} X_{n-p} = E_n, \quad \forall n, \quad (5)$$

where $\{E_n\}$ is a zero-mean white noise process with the variance $\sigma^2 > 0$ [31, Def. 3.1.2]. In the source-filter signal

model, (5) represents the process of passing the excitation noise $\{E_n\}$ through an all-pole filter with the coefficients a_1, a_2, \dots, a_{p+1} , where $a_1 = 1$ is assumed without the loss of generality [2, Ch. 4].

In terms of real-world signal modeling, (5) can be reformulated for a particular observation $\mathbf{x} \in \mathbb{R}^N$ as

$$\sum_{i=1}^{p+1} a_i x_{n+1-i} = e_n, \quad a_1 = 1, \quad n = 1, \dots, N+p. \quad (6)$$

The vector \mathbf{x} is zero-padded to its new length $N+p$, such that (6) is correctly defined. The definition in (6) is in close relationship with linear convolution and in accordance with the convention of the `lpc` function in Matlab. From the perspective of model fitting, the vector $\mathbf{e} \in \mathbb{R}^{N+p}$ is called the *residual error* [1, Sec. 8.2.2]. Given the observed signal \mathbf{x} and the order p , the AR model is estimated by

$$\arg \min_{\mathbf{a}} \frac{1}{2} \|\mathbf{e}(\mathbf{a}, \mathbf{x})\|^2. \quad (7)$$

In (7), we denote $\mathbf{a} = [1, a_2, a_3, \dots, a_{p+1}]^\top$ (i.e., we inherently minimize subject to $a_1 = 1$), and $\mathbf{e} = [e_1, e_2, \dots, e_{N+p}]^\top$ is defined in (6) as a function of both the signal \mathbf{x} and the coefficients \mathbf{a} . This can effectively be solved, for example, by using the autocorrelation method and the Levinson–Durbin algorithm [32], [33].

We define the regularized autoregressive model using an optimization formulation as follows:

$$\arg \min_{\mathbf{a}, \mathbf{x}} \{Q(\mathbf{a}, \mathbf{x}) = \frac{1}{2} \|\mathbf{e}(\mathbf{a}, \mathbf{x})\|^2 + \lambda_C f_C(\mathbf{a}) + \lambda_S f_S(\mathbf{x})\}, \quad (8)$$

where we assume $\lambda_C, \lambda_S \geq 0$, and f_C, f_S are (preferably) convex lower semicontinuous functions.

The idea behind (8) is that the AR nature of the signal is preserved by minimizing the residual error as in (7) but, at the same time, possible priors on the AR coefficients \mathbf{a} and the signal \mathbf{x} are incorporated via the functions f_C and f_S , respectively.

The audio inpainting task corresponds to problem (8) with $f_C = 0$, and f_S being the indicator function of the set Γ_{inp} of feasible signals; see also (1). In such a situation, the hard constraints $M_{\text{R}}\mathbf{x} = M_{\text{R}}\mathbf{y}$ can be directly incorporated in the noise-minimization term, which is more effective compared to working directly with (8) in practice [11]. A similar model is the HOSpLP framework for audio inpainting [23], where the coefficient estimation is regularized solely by $f_C(\mathbf{a}) = \|\mathbf{a}\|_1$, or even by a non-convex sparsity penalty [24]. In contrast to (8), HOSpLP further allows utilizing a different norm for the residual \mathbf{e} , which is assumed to be more suitable, e.g., to model voiced speech (in such a case, the source in the source-filter model is a pulse train rather than white noise).

Another reason for the AR model regularization may be numerical stability. Without a regularization of the AR coefficients, the overall objective function and SNR may improve, the AR coefficients themselves may grow disproportionately (for example, a difference of the order of 10^4 compared with the clean signal AR coefficients may appear). Using the parameter $\lambda_C > 0$, this numerically undesirable behavior can be controlled.

III. ALGORITHMIC APPROACH

Suppose the functions f_C, f_S are convex; it follows that the problem (8) poses a biconvex optimization, meaning that although (8) as a whole is non-convex, minimizations of $Q(\mathbf{a}, \mathbf{x})$ over \mathbf{a} and over \mathbf{x} separately represent convex problems. Such cases appear frequently in the literature [6], [34], and the problem is typically treated via the Alternate Convex Search (ACS) [35, Sec. 4.2.1]. Note that the same update scheme can also be obtained from the Alternating Direction Method of Multipliers, when applied to the biconvex problem (8), see [36, Sec. 9.2].

A. Alternate Convex Search Algorithm

Statements regarding the convergence of the ACS are generally not possible, see also [11, Appendix B]. Thanks to biconvexity, however, at least the convergence of the objective values can be guaranteed, i.e., of the sequence $\{Q(\mathbf{a}^{(i)}, \mathbf{x}^{(i)}) \mid i = 1, 2, \dots\}$. However, the limit of the sequence may not be the global minimum of $Q(\mathbf{a}, \mathbf{x})$. Some practical convergence properties can be stated when the sequence $\{(\mathbf{a}^{(i)}, \mathbf{x}^{(i)})\}$ is contained in a compact set, which could be enforced, for example, by defining f_C, f_S as indicator functions [37], and if both the individual convex sub-problems have unique solutions. Under these assumptions, the ACS sequence has at least one accumulation point and all the accumulation points are stationary points of $Q(\mathbf{a}, \mathbf{x})$ [35, Thm. 4.9, Corr. 4.10].

In both the subproblems of minimizing $Q(\mathbf{a}, \mathbf{x})$ over \mathbf{a} and over \mathbf{x} , the other variable is constant, which allows omitting also the respective part of the objective function in (8) and simplify the updates to

$$\mathbf{a}^{(i)} = \arg \min_{\mathbf{a}} \left\{ \frac{1}{2} \|\mathbf{e}(\mathbf{a}, \mathbf{x}^{(i-1)})\|^2 + \lambda_C f_C(\mathbf{a}) \right\}, \quad (9a)$$

$$\mathbf{x}^{(i)} = \arg \min_{\mathbf{x}} \left\{ \frac{1}{2} \|\mathbf{e}(\mathbf{a}^{(i)}, \mathbf{x})\|^2 + \lambda_S f_S(\mathbf{x}) \right\}. \quad (9b)$$

In the following subsections, the ways to solve the subproblems (9a) and (9b) are discussed. As will be demonstrated, it turns out that the bottleneck is the computational complexity. Therefore, the possibilities of accelerating the ACS procedure will also be discussed.

B. Dealing with the sub-problems

In the convex setting and with nonzero f_C, f_S , the problems (9a) and (9b) can be addressed via proximal splitting methods [37]. Each of the problems consists of a sum of two convex functions, the quadratic AR model error and a possibly non-smooth penalty f_C or f_S . The key concept of the proximal splitting is to reach the global optimum by repetitive minimization using gradients or the so-called proximal operators related to individual summands.

The proximal operator of a function f is another function on the same space, defined as¹ $\text{prox}_f(\mathbf{u}) = \arg \min_{\mathbf{v}} \{ \frac{1}{2} \|\mathbf{v} - \mathbf{u}\|^2 + f(\mathbf{v}) \}$. Among the typical examples is the projection onto a convex set C , which is the proximal operator of the

¹If the function f is convex lower semicontinuous, the minimization has a unique solution, thus the corresponding proximal operator is well defined.

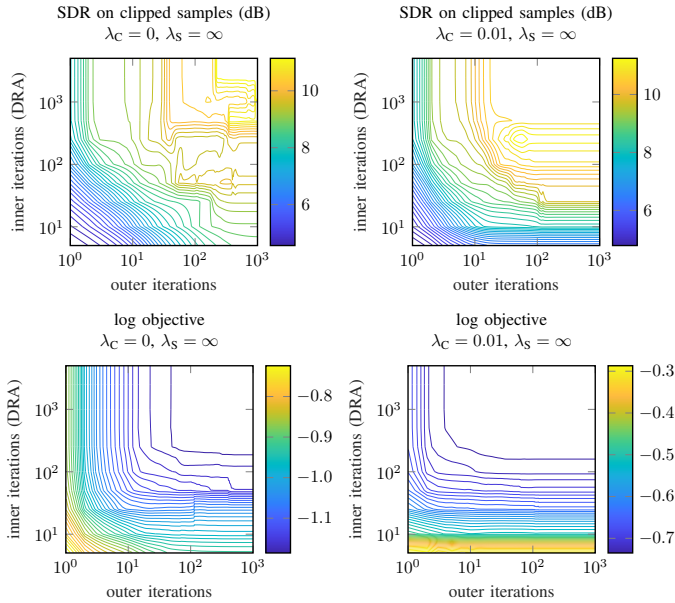


Fig. 2. Trade-off between the count of inner and outer iterations. The problem being solved is the consistent declipping of a single signal frame, i.e., the problem (13) with $\lambda_S = \infty$ and variable λ_C . The signal segment length is 2048 samples, the model order is $p = 512$. For reference, the SDR of the clipped signal is 4.3 dB.

The main conclusion from this experiment is that for large numbers of ACS iterations, the result no longer improves. Especially in the case of AR model regularization (plots in the right column of Fig. 2 with $\lambda_C = 0.01$), no large improvement is observed from 10 iterations on. This is in correspondence with [11], where even a single iteration was considered. This also means that the unknown convergence properties, as discussed in Sec. III-A, seem not very limiting, at least in our setup. Contrarily, the number of inner iterations (i.e., the precision in solving the subproblems (9)) appears crucial. This interpretation stems from the observation that both the SDR and the objective function in the plots in Fig. 2 vary significantly in the vertical direction (w.r.t. the number of inner iterations).

B. Progression towards oracle coefficients?

The SDR values in the previous experiment suggest a good applicability of the regularized AR model for audio declipping, meaning that the resulting audio signal resembles the undistorted original. This section aims at answering the subsequent question, whether also the sequence of AR coefficients $\{\mathbf{a}^{(i)}\}$ generated by the ACS converges towards the AR coefficients of the clean signal.

To investigate this subject, a declipping experiment according to (13) is performed, where, in addition to objective and SDR, we track the evolution of the (regularized) AR coefficients in the iterations of the ACS. This allows a comparison with the coefficients of the undistorted signal.

The results of the experiment are presented in Fig. 3. The conclusion is that it is possible that the AR coefficients converge over iterations (usually the relative difference between iterations decreases). However, it appears that the coefficients

of the undamaged signal are not the potential limit, because the norm of the difference to this *actual* solution (plotted in the third graph) usually does not decrease.

C. Regularization

After demonstrating that the proposed algorithmic approach allows fitting the regularized AR model, the aim is to dig deeper in the declipping application. A common problem in regularized inverse problems is the trade-off related to the regularization strength, typically governed by a scalar parameter. In the case of the generic problem (8), or the particular declipping formulation (13), there are two regularization parameters λ_C, λ_S , which may significantly affect the reconstruction quality.

To evaluate the effect of the regularization, an experiment is performed, where clipped signals are reconstructed using all three strategies (inpainting, GLP, declipping), for different choices of λ_C and λ_S in the case of the proposed declipping approach. The results, in terms of SDR, are presented in Table I. The observation is that the results are not very sensitive to the choice of λ_S , even though the declipping strategy (i.e., $\lambda_S > 0$) leads to a minor improvement over inpainting or GLP. Regarding λ_C , the choice to regularize the AR coefficients (i.e., $\lambda_C > 0$) also improves the reconstruction quality; however, the regularization must be chosen carefully in order not to be overly strong (see the results for $\lambda_C = 10^{-1}$).

D. Comparison with methods from audio declipping survey

To provide a context for the reconstruction quality reachable by the regularized AR model, our last experiment compares the results with the survey [9]. The same set of 10 musical signals is used and degraded in the same way, i.e., hard-clipped with the clipping level chosen according to a given input SDR (5, 7, 10 and 15 dB).

The order of the regularized AR model is $p = 512$, with the window length set to $w = 8192$. The inner iterations are solved using the FFT-accelerated DRA with 1 000 iterations, and the whole ACS algorithm has 5 outer iterations with signal extrapolation (see Appendix A-B).

First, the results are evaluated using SDR (see equation (14)) and shown in Fig. 4a. More precisely, Fig. 4a shows the values ΔSDR , defined as the improvement of SDR of the recovered signal over the SDR of the clipped signal (also denoted as the input SDR).

The effect of the regularization of the AR coefficients (λ_C) in the case of inpainting and GLP appears to be rather negative in terms of the quality of the reconstruction. On the other hand, it is beneficial in the case of declipping for input SDR < 15 dB. An important observation is that GLP does *not* perform better than inpainting, and it outperforms declipping only for a very low input SDR. This suggests that if time-domain consistency is essential, the declipping strategy is a better choice; if computational complexity is the priority, then the inpainting strategy is sufficient. For a lower input SDR, the results are positively affected also by increasing $\lambda_S > 0$.

Note that for methods inconsistent with the reliable observation, post-processing methods exist to leverage the reliable

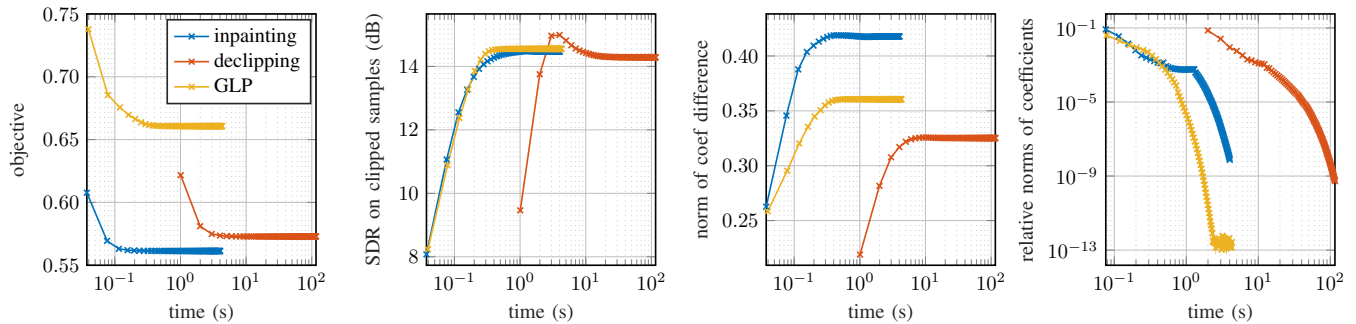


Fig. 3. Analysis of convergence of the three main competitors towards the clean signal and oracle AR coefficients. In this particular case, 2048-sample-long realization of an AR process of the order $p = 128$ was used as the clean signal and clipped at 0.2 times the peak value (this corresponds to an SDR of 4.6 dB on clipped samples). For reconstruction, we set $\lambda_C = 0.1$ and $\lambda_S = \infty$ (i.e., declipping is in its consistent variant). All three algorithms run for 100 outer iterations and 1 000 inner iterations of the (non-accelerated) DRA. Note that the objective functions (the first graph) are in general different for different algorithms due to the choices of the parameters λ_C, λ_S .

TABLE I
MEAN SDR (dB) FROM 10 SIGNALS, EACH INITIALLY DEGRADED BY CLIPPING AT AN INPUT SDR OF 10 dB. THE PARAMETERS USED IN THE RECONSTRUCTION ARE $w = 2048$, $p = 512$, 10 OUTER ITERATIONS AND 1 000 INNER ITERATIONS. FOR EACH ALGORITHM (DECLIPPING, GLP, INPAINTING), THE MAXIMAL VALUE (PRIOR TO ROUNDING) IS HIGHLIGHTED.

	$\lambda_C = 0$	$\lambda_C = 10^{-6}$	$\lambda_C = 10^{-5}$	$\lambda_C = 10^{-4}$	$\lambda_C = 10^{-3}$	$\lambda_C = 10^{-2}$	$\lambda_C = 10^{-1}$
declipping, $\lambda_S = \infty$	22.9	23.5	23.5	23.7	24.3	23.1	19.1
declipping, $\lambda_S = 100$	22.9	23.5	23.5	23.7	24.3	23.1	19.1
declipping, $\lambda_S = 10$	22.9	23.5	23.6	23.7	24.3	23.0	18.9
declipping, $\lambda_S = 1$	22.4	23.1	23.1	23.3	23.8	22.1	18.0
GLP	22.4	22.4	22.4	22.5	22.6	21.9	18.0
inpainting	23.4	23.2	23.3	23.5	23.9	22.1	17.7

samples and increase the objective quality [10]. In the case of declipping with the regularized AR model, this is the case of $0 < \lambda_S < \infty$. Since [10] presented promising results in terms of objective perceptual metrics, we apply this strategy also to the signals restored using the regularized AR model in the declipping setting. In particular, we use the “crossfade reliable” update with default parameters taken from the accompanying repository².

The original, as well as the post-processed signals are evaluated using the PEMO-Q and PEAQ objective methods and shown in Fig. 4b and 4c, respectively. In terms of PEMO-Q, the post-processing *decreases* the objective quality in most cases. This effect is visible also in the case of the reference methods for a lower input SDR. Regarding PEAQ, crossfading the reliable samples improves the declipping results; however, the improvement is not as significant as in the case of some of the reference methods. In general, the observations are similar as in the case of Δ SDR in Fig. 4a; however, the benefit of the regularization of the AR coefficients ($\lambda_C > 0$) is questionable.

The overall outcome of the experiment is that compared to the methods tested in the survey [9], the regularized AR model scores among the best and offers an alternative to the state-of-the-art methods. However, no significant improvement of the state of the art is observed.

Furthermore, the regularization of the signal ($\lambda_S > 0$) was expected to be clearly beneficial, but it led to outperforming the other AR-based competitors (inpainting, GLP) for a higher input SDR only. A hypothesis is that although consistency

in the time domain (satisfying the clipping conditions) can be approached with $\lambda_S > 0$ and even guaranteed in the case $\lambda_S = \infty$, we are forced to numerically solve the subproblem (9b), which carries risks (only approximate solution due to the limited number of iterations, possible insufficient bias of the declipped samples).

E. Software, data & reproducible research

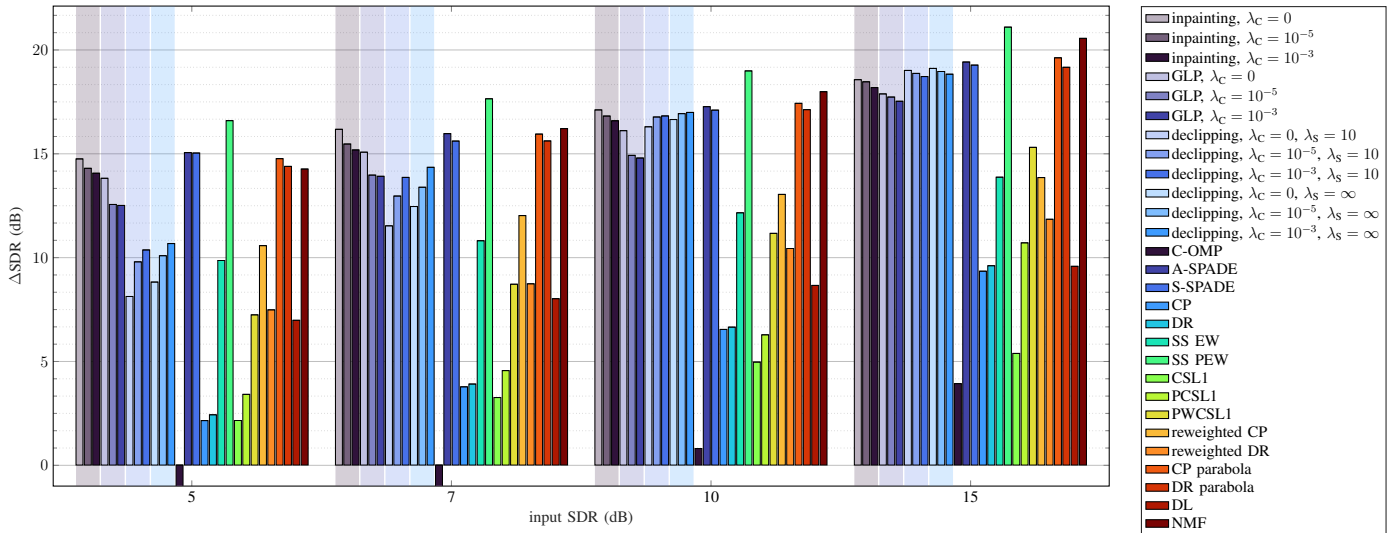
Our software is available on <https://github.com/ondrejmkry/RegularizedAutoregression>. We run it using Matlab R2021a and R2023a.

To obtain results via the basic Janssen method (i.e., effectively audio inpainting) we used parts of the SMALLbox [40]. The same applies to the GLP method [15], whose fundamental step coincides with that of the Janssen method. The FFT-based acceleration of the Douglas–Rachford algorithm was taken from [39]. When comparing our results with those of the reference methods from the survey [9], we took directly the reported and publicly available signals from the accompanying repository https://github.com/rajmic/declipping2020_codes. Finally, in the case of the methods based on the “replace reliable” strategy, we downloaded them from the webpage <https://rajmic.github.io/declipping2020/>.

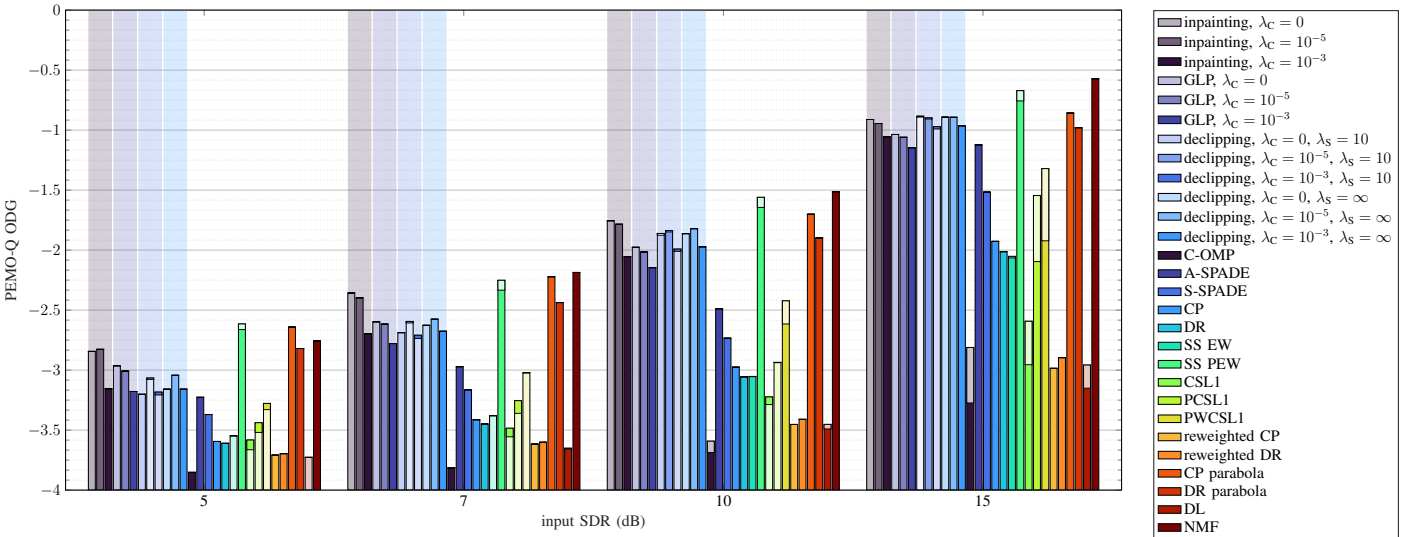
V. CONCLUSION

We have developed a comprehensive and general framework alongside its associated optimization problem and algorithm which encompasses the previous attempts to enhance the basic popular AR model. The framework allows to constrain the

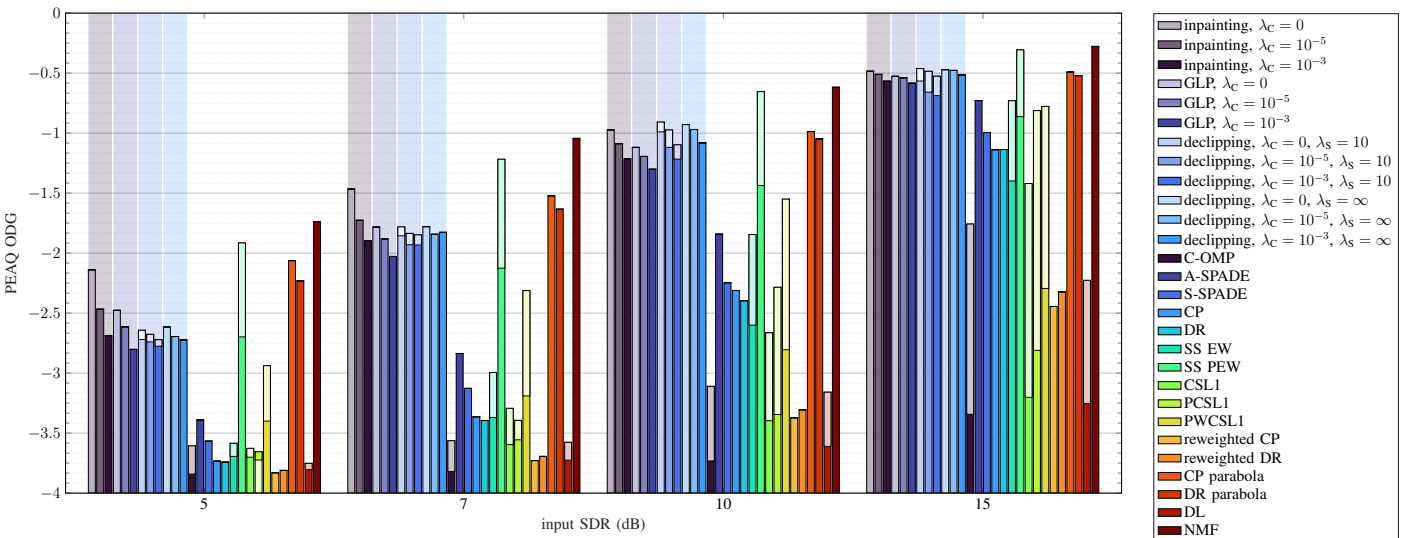
²https://github.com/rajmic/declipping2020_codes



(a) comparison in terms of Δ SDR, i.e. the improvement of SDR over the clipped signal



(b) comparison in terms of PEMO-Q



(c) comparison in terms of PEAQ

Fig. 4. Comparison of the regularized AR model with the methods from the survey [9]. Results of the methods based on the AR model, treated in this article, are indicated with a background color. In the case of PEMO-Q and PEAQ, results using the “replace reliable” strategy from [10] are shown using stacked bars. For each algorithm which may produce signals inconsistent with the reliable samples, the cross-faded strategy is applied and the updated result is shown in lighter shade.

signal values in the time domain or to regularize the AR coefficients. We thoroughly discussed the computational implications of this algorithm and assessed the impact of several enhancements on its performance in terms of computational load.

The experiments focused on the problem of audio declipping as a natural use case of the proposed framework, where degraded signal samples are constrained to exceed a known clipping level. We have demonstrated good applicability of the regularized AR method and conducted a comparison with current state-of-the-art methods. We have proven the competitiveness of the proposed solution, particularly in the context of signals that have experienced mild clipping.

We have also pointed out the main drawback of the regularized AR modeling, which is the computational complexity. In the presented declipping application, this was mainly due to the choice of rather large dimensionality of both the coefficient and signal domains of the central problem (13). While we have proposed several strategies allowing a substantial reduction of the computational times, further acceleration for audio processing applications remains a challenge.

Regarding other future possibilities, the relationship of the AR coefficients and the signal, invoked by the minimization (7), could be relaxed such that the noise (error) is shaped according to the masking properties of the human ear [2, Sec. 4.1]. Such modification could lead to higher perceptual quality of the solution when using the regularized AR model in the reconstruction of degraded audio signals.

APPENDIX A ACCELERATION

This appendix presents different strategies to accelerate the solution to the problem (13), following section III-B. Two different approaches are presented in sections A-A and A-B and evaluated numerically in section A-C.

A. Progressive sub-iteration counts

Inspired by the trade-off behavior between outer and inner iteration counts (see Sec. IV-A and Fig. 2), we propose a progressive strategy of choosing the inner iteration counts. Since it appears from the experiments that good precision is necessary for a satisfactory estimation in a single outer iteration, the idea is to “spare” some inner iterations only in the beginning of the ACS while keeping the necessary precision in the final iterations, where the resulting signal is sought. More specifically, a logarithmic distribution of the inner iterations is proposed. Denote I the number of outer iterations and $N^{(i)}$ the number of inner iterations for $i = 1, \dots, I$. For the chosen values of $n^{(1)}$ and $n^{(I)}$, the proposed scheme is

$$N^{(i)} = 10^{n^{(1)} + \frac{i-1}{I-1}(n^{(I)} - n^{(1)})}, \quad (15)$$

or, in Matlab notation³,

$$[N^{(1)}, \dots, N^{(I)}] = \text{logspace}(n^{(1)}, n^{(I)}, I). \quad (16)$$

In particular, it holds $N^{(1)} = 10^{n^{(1)}}$ and $N^{(I)} = 10^{n^{(I)}}$.

³<https://www.mathworks.com/help/matlab/ref/logspace.html>

B. Extrapolation and line search in the subproblems

Although the acceleration of DRA helps to significantly reduce the computational time, especially in the signal-estimation subproblem, the whole ACS algorithm remains very demanding. As outlined in Sec. IV-A, the reason is that an accurate solution of the subproblems is necessary to achieve satisfactory results of the ACS algorithm.

In response to this observation, we propose several extrapolation strategies for the subproblems, as well as for the whole ACS:

1) extrapolate the coefficient update:

- compute $\mathbf{a}^{(i-\frac{1}{2})}$ as a solution to (9a),
- extrapolate $\mathbf{a}^{(i)} = (1 + \tau_C)\mathbf{a}^{(i-\frac{1}{2})} - \tau_C\mathbf{a}^{(i-1)}$ for the chosen step size $\tau_C > 0$,

2) extrapolate the signal update:

- compute $\mathbf{x}^{(i-\frac{1}{2})}$ as a solution to (9b),
- extrapolate $\mathbf{x}^{(i)} = (1 + \tau_S)\mathbf{x}^{(i-\frac{1}{2})} - \tau_S\mathbf{x}^{(i-1)}$ for the chosen step size $\tau_S > 0$,

3) line search:

- compute $\mathbf{a}^{(i-\frac{1}{2})}$ as a solution to (9a),
- compute $\mathbf{x}^{(i-\frac{1}{2})}$ as a solution to (9b) with $\mathbf{a}^{(i-\frac{1}{2})}$ fixed instead of $\mathbf{a}^{(i)}$,
- choose $\hat{\tau}$ such that

$$\hat{\tau} = \arg \min_{\tau \geq 0} Q(\mathbf{a}(\tau), \mathbf{x}(\tau)), \quad (17)$$

where $\mathbf{a}(\tau) = (1 + \tau)\mathbf{a}^{(i-\frac{1}{2})} - \tau\mathbf{a}^{(i-1)}$
and $\mathbf{x}(\tau) = (1 + \tau)\mathbf{x}^{(i-\frac{1}{2})} - \tau\mathbf{x}^{(i-1)}$,

- extrapolate as $\mathbf{a}^{(i)} = \mathbf{a}(\hat{\tau})$ and $\mathbf{x}^{(i)} = \mathbf{x}(\hat{\tau})$.

A problem of the line search strategy is the non-convexity⁴ of the composed problem (8). Thus, no guarantee of finding a minimum with respect to the considered half-line is at hand in general. However, our empirical examples show that an improvement of the objective via sampling a suitable selection of the half-line is possible.

C. Numerical experiment

The acceleration strategies proposed above have been tested on a declipping problem with an input SDR of 10 dB (see Sec. IV for details). As the baseline serves the ACS algorithm with $I = 10$ outer iterations and DRA as the sub-solver with 1 000 iterations. The accelerated versions include:

- FFT-based acceleration of the DRA [39].
- Progressive iteration according to Sec. A-A with 100 iterations of DRA in the first iteration of ACS ($n^{(1)} = 2$, $N^{(1)} = 100$) and 1 000 iterations of DRA in the last iteration of ACS ($n^{(10)} = 3$, $N^{(10)} = 1 000$), spaced logarithmically.

⁴In the context of the line search, the important observation is that the objective is non-convex over the half-line under consideration. The only exception is a discrete set of search directions, as can be observed in an illustrative example of $Q(a, x) = a \cdot x$ with the scalars a, x .

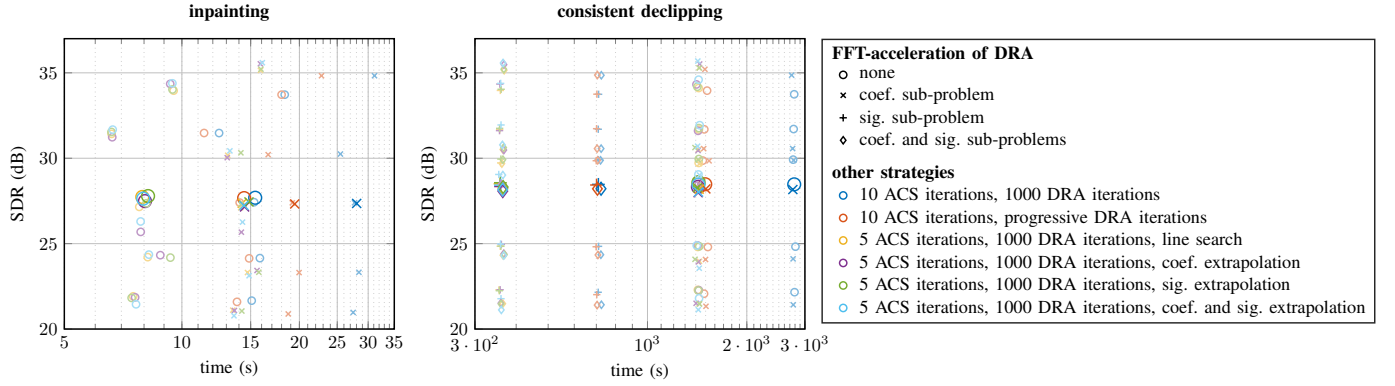


Fig. 5. Comparison of the acceleration options for the window length $w = 8192$ samples and the AR model order $p = 512$. The smaller and lighter points represent individual reconstructions in the experiment, the larger points are the mean values.

- Extrapolation according to Sec. A-B with the following extrapolation steps for the signal and/or the AR model coefficients in the iteration i of $I = 5$:

$$\mathbf{x}^{(i)} = \mathbf{x}^{(i-\frac{1}{2})} + \frac{I-i}{I-1}(\mathbf{x}^{(i-\frac{1}{2})} - \mathbf{x}^{(i-1)}), \quad (18a)$$

$$\mathbf{a}^{(i)} = \mathbf{a}^{(i-\frac{1}{2})} + 2\frac{I-i}{I-1}(\mathbf{a}^{(i-\frac{1}{2})} - \mathbf{a}^{(i-1)}). \quad (18b)$$

In line with A-B, we have in the i -th iteration $\tau_S = \frac{I-i}{I-1}$ (i.e., the extrapolation step length decreases from $\tau_S = 1$ in the first iteration to $\tau_S = 0$, meaning no extrapolation in the I -th iteration). Similarly, we have $\tau_C = 2\frac{I-i}{I-1}$.

- Line search according to Sec. A-B, considering only $\tau \in [0.0001, 100]$ for computational reasons.

To evaluate the acceleration, the computation time is tracked for the considered ways of estimating the AR coefficients and the declipped signal, together with the reconstruction quality. The experiment was performed on a PC with the Intel Core i7 3.40 GHz processor, 32 GB RAM.

The numerical results for five short signals⁵ are presented in Fig. 5 and 7. Fig. 5 shows the individual reconstructions in the time-quality plane, where the reconstruction quality is measured using SDR. In this plot, a suitable acceleration strategy should have its data points to the left from the baseline (meaning lower computational time) and not below the baseline (meaning the same or a better reconstruction quality). The same data are shown in Fig. 7 in a different manner. There, the decrease in computational time (i.e., time gain) and decrease in SDR (i.e., performance loss) are shown together as stacked bars for each acceleration strategy. Furthermore, this plot shows the data for different orders of the AR model and different window lengths, since the acceleration rate is supposed to depend on the problem size. Note that all the values shown in Fig. 7 are relative with respect to the baseline values shown in Fig. 6.

The conclusion from this experiment is that the most beneficial option is to use the FFT-accelerated DRA in both sub-problems of (9). The computation time is greater merely in some cases of inpainting and GLP. Regarding the reconstruction quality, the PEAQ ODG values do not show

any difference, and the related graphical representation is thus omitted. In terms of PEAQ ODG or SDR, a loss of reconstruction quality is observed; mainly in cases including the extrapolation of the estimated AR model. A less significant quality loss is observed in the line search case and signal extrapolation.

As a compromise between acceleration and reconstruction quality loss, the experiment favors using 1000 inner iterations of the FFT-accelerated DRA with extrapolation of the signal update according to (18a) (see Fig. 5 and 7).

APPENDIX B PROXIMAL OPERATORS

In this appendix, we treat in more detail the components utilized to fit the regularized AR model in the case of audio declipping, i.e., to solve the problem (13). In (12), we already have introduced the proximal operators of the error term appearing in (13). For the sparsity term $\lambda_C \|\mathbf{a}\|_1$, the corresponding proximal operator $\text{prox}_{\lambda_C \|\cdot\|_1} = \text{prox}_{\lambda_C \|\cdot\|_1}$ is the soft thresholding [38, Ex. 6.8]:

$$\left(\text{prox}_{\lambda_C \|\cdot\|_1}(\mathbf{a})\right)_n = \begin{cases} a_n - \lambda_C, & a_n \geq \lambda_C, \\ 0, & |a_n| < \lambda_C, \\ a_n + \lambda_C, & a_n \leq -\lambda_C. \end{cases} \quad (19)$$

Regarding the signal regularization $\lambda_S d_{\Gamma_{\text{declip}}}(\mathbf{x})^2/2$, we have for $\lambda_S < \infty$ [38, Ex. 6.65]

$$\text{prox}_{\lambda_S d_{\Gamma_{\text{declip}}}(\mathbf{x})^2/2}(\mathbf{x}) = \frac{\lambda_S}{\lambda_S + 1} \text{proj}_{\Gamma_{\text{declip}}}(\mathbf{x}) + \frac{1}{\lambda_S + 1} \mathbf{x}. \quad (20)$$

To cover also the consistent case with $\mathbf{x} \in \Gamma_{\text{declip}}$, we allow the choice $\lambda_S = \infty$, which is interpreted as replacing $\lambda_S d_{\Gamma_{\text{declip}}}(\mathbf{x})^2/2$ with the indicator function $\iota_{\Gamma_{\text{declip}}}(\mathbf{x})$. The corresponding proximal operator is the projection [38, Thm. 6.24]

$$\text{prox}_{\iota_{\Gamma_{\text{declip}}}}(\mathbf{x}) = \text{proj}_{\Gamma_{\text{declip}}}(\mathbf{x}). \quad (21)$$

While (21) is the limit case of (20) for $\lambda_S \rightarrow \infty$, our Matlab implementation treats the two cases individually.

ACKNOWLEDGMENT

The work was supported by the Czech Science Foundation (GAČR) Project No. 23-07294S.

⁵The test signals are single-instrument recordings extracted from the set based on the EBU SQAM database, as described in Sec. IV, and shortened to a length of 0.6s.

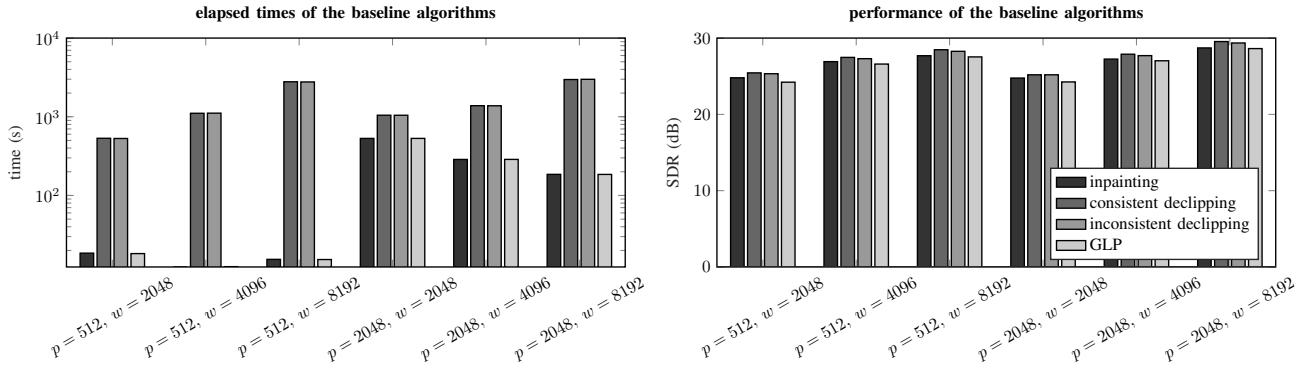


Fig. 6. Baseline elapsed times and performance in terms of SDR using 10 ACS iterations and 1000 DRA iterations with no acceleration strategy.

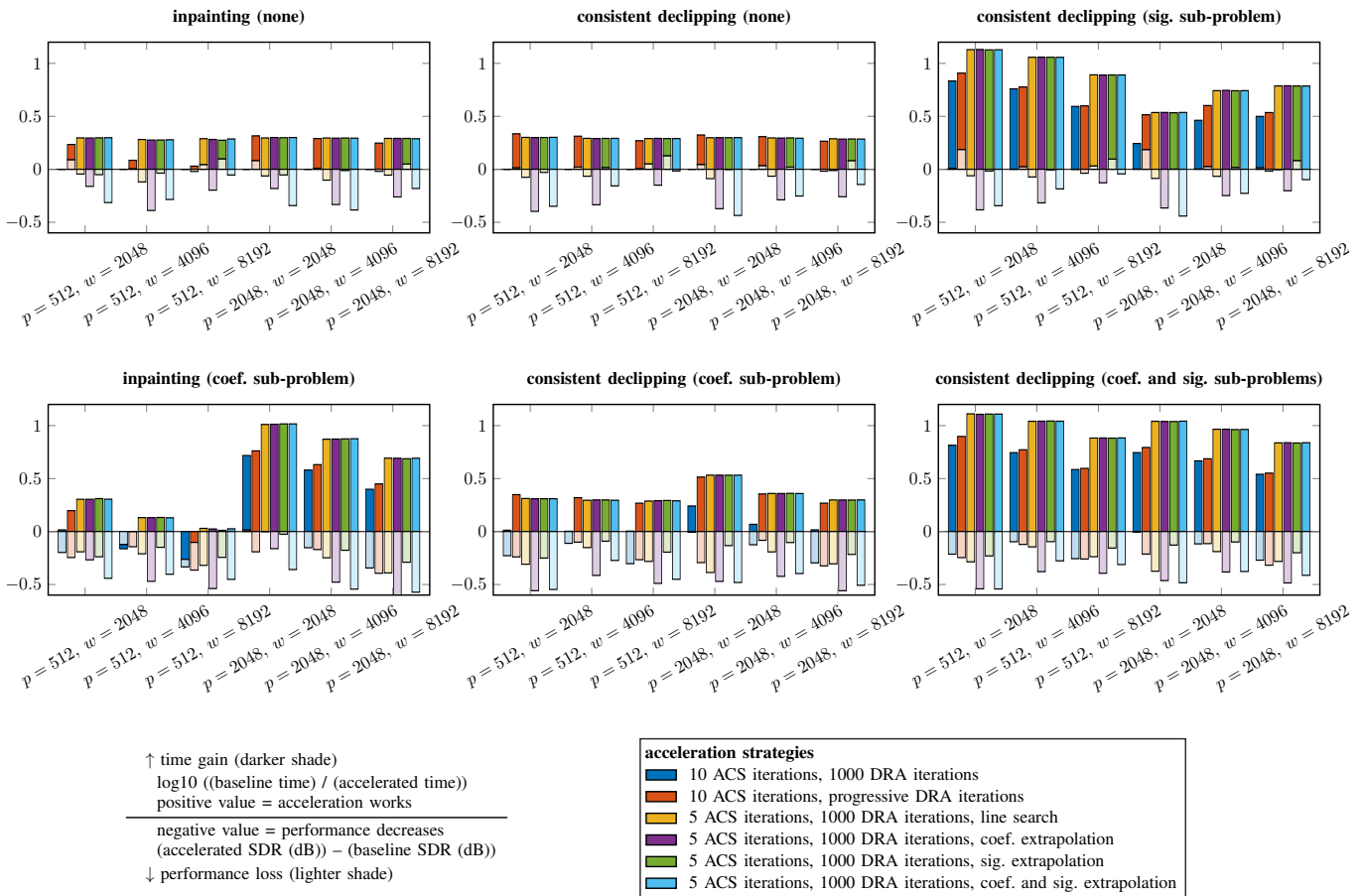


Fig. 7. Performance of the acceleration strategies for an input SDR of 10 dB, dependent on the window length w and the AR model order p . Color coding is the same in the whole figure and is identical to Fig. 5. FFT-acceleration of the DRA in the coefficient and signal sub-problems (9a) and (9b) is indicated in brackets above the individual plots. Positive time gain (darker-shade bar has a value above 0) means that the acceleration truly reduces computation time. A positive performance loss (the lighter-shade bar has a value below 0) means that the acceleration causes a drop in the reconstruction SDR. For the baseline time and SDR, see Fig. 6.

REFERENCES

- [1] U. Zölzer, *DAFX: Digital Audio Effects*, 2nd ed., U. Zölzer, Ed. Wiley, 2011.
- [2] A. Spanias, T. Painter, and V. Atti, *Audio Signal Processing and Coding*. John Wiley & Sons, Inc., 12 2005.
- [3] R. S. Tsay, *Analysis of financial time series*, 2nd ed. Hoboken, N.J: Wiley, 2005.
- [4] H. Akaike, *Autoregressive Model Fitting for Control*. New York, NY: Springer New York, 1998, pp. 153–170. [Online]. Available: https://doi.org/10.1007/978-1-4612-1694-0_12
- [5] T. Takahashi, K. Konishi, and T. Furukawa, “Hankel structured matrix rank minimization approach to signal declipping,” in *21st European Signal Processing Conference (EUSIPCO 2013)*, Sep. 2013, pp. 1–5.
- [6] P. Závíška, P. Rajmic, and O. Mokry, “Multiple Hankel matrix rank minimization for audio inpainting,” in *2023 46th International Conference on Telecommunications and Signal Processing (TSP)*. IEEE, jul 2023.
- [7] W. Etter, “Restoration of a discrete-time signal segment by interpolation based on the left-sided and right-sided autoregressive parameters,” *IEEE Transactions on Signal Processing*, vol. 44, no. 5, pp. 1124–1135, 1996.
- [8] S. Kitić, L. Jacques, N. Madhu, M. Hopwood, A. Spriet, and C. De Vleeschouwer, “Consistent iterative hard thresholding for signal declipping,” in *Acoustics, Speech and Signal Processing (ICASSP), 2013 IEEE International Conference on*, May 2013, pp. 5939–5943.
- [9] P. Závíška, P. Rajmic, A. Ozerov, and L. Rencker, “A survey and an extensive evaluation of popular audio declipping methods,” *IEEE Journal of Selected Topics in Signal Processing*, vol. 15, no. 1, pp. 5–24, 2021.
- [10] P. Závíška, P. Rajmic, and O. Mokry, “Audio declipping performance enhancement via crossfading,” *Signal Processing*, vol. 192, p. 108365, 2022. [Online]. Available: <https://www.sciencedirect.com/science/article/pii/S0165168421004023>
- [11] A. J. E. M. Janssen, R. N. J. Veldhuis, and L. B. Vries, “Adaptive interpolation of discrete-time signals that can be modeled as autoregressive processes,” *IEEE Trans. Acoustics, Speech and Signal Processing*, vol. 34, no. 2, pp. 317–330, Apr. 1986.
- [12] L. Oudre, “Interpolation of missing samples in sound signals based on autoregressive modeling,” *Image Processing On Line*, vol. 8, pp. 329–344, Oct. 2018.
- [13] O. Mokry and P. Rajmic, “Audio inpainting: Revisited and reweighted,” *IEEE/ACM Transactions on Audio, Speech, and Language Processing*, vol. 28, pp. 2906–2918, 2020.
- [14] O. Mokry and P. Rajmic, “On the use of autoregressive methods for audio inpainting,” Mar. 2024. [Online]. Available: <https://arxiv.org/abs/2403.04433>
- [15] L. Atlas and P. Clark, “Clipped-waveform repair in acoustic signals using generalized linear prediction,” U.S. patentus US 8 126 578 B2, Sep. 26, 2012. [Online]. Available: <https://patents.google.com/patent/US8126578>
- [16] I. Kauppinen and J. Kauppinen, “Reconstruction method for missing or damaged long portions in audio signal,” *Journal of the Audio Engineering Society*, vol. 50, no. 7/8, pp. 594–602, 2002. [Online]. Available: <http://www.aes.org/e-lib/browse.cfm?elib=11068>
- [17] I. Kauppinen and K. Roth, “Audio Signal Extrapolation – Theory and Applications,” in *Proceedings of the 5th International Conference on Digital Audio Effects (DAFx-02)*, Hamburg, Germany, Sep. 2002, pp. 105–110. [Online]. Available: http://www2.hsu-hh.de/ant/dafx2002/papers/DAFX02_Kauppinen_Roth_signal_extrapolation.pdf
- [18] P. A. A. Esquef, V. Välimäki, K. Roth, and I. Kauppinen, “Interpolation of long gaps in audio signals using the warped Burg’s method,” in *Proceedings of the 6th International Conference on Digital Audio Effects (DAFx-03)*, London, UK, Sep. 2003, pp. 18–23.
- [19] K. Roth, I. Kauppinen, P. A. A. Esquef, and V. Välimäki, “Frequency warped Burg’s method for AR-modeling,” in *2003 IEEE Workshop on Applications of Signal Processing to Audio and Acoustics (IEEE Cat. No.03TH8684)*, ser. ASPAA-03. IEEE, 2003.
- [20] V. Vesely and J. Tonner, “Sparse parameter estimation in overcomplete time series models,” *Austrian Journal of Statistics*, vol. 35, pp. 371–378, 2006. [Online]. Available: <http://www.stat.tugraz.at/AJS/ausg062+3/062Vesely.pdf>
- [21] D. Giacobello, M. G. Christensen, J. Dahl, S. H. Jensen, and M. Moonen, “Joint estimation of short-term and long-term predictors in speech coders,” in *2009 IEEE International Conference on Acoustics, Speech and Signal Processing*. IEEE, Apr. 2009.
- [22] D. Giacobello, M. G. Christensen, M. N. Murthi, S. H. Jensen, and M. Moonen, “Sparse linear prediction and its applications to speech processing,” *IEEE Transactions on Audio, Speech, and Language Processing*, vol. 20, no. 5, pp. 1644–1657, Jul. 2012.
- [23] B. D. Dufera, K. Eneman, and T. van Waterschoot, “Missing sample estimation based on high-order sparse linear prediction for audio signals,” in *2018 26th European Signal Processing Conference (EUSIPCO)*. IEEE, Sep. 2018.
- [24] B. D. Dufera, E. Adugna, K. Eneman, and T. van Waterschoot, “Restoration of click degraded speech and music based on high order sparse linear prediction,” in *2019 IEEE AFRICON*. IEEE, Sep. 2019.
- [25] T. Tanaka, K. Yatabe, M. Yasuda, and Y. Oikawa, “APPLADE: Adjustable plug-and-play audio declipper combining DNN with sparse optimization,” in *2022 IEEE International Conference on Acoustics, Speech and Signal Processing (ICASSP)*. IEEE, may 2022.
- [26] Y. Kwon and J.-W. Choi, “Speech-declipping transformer with complex spectrogram and learnable temporal features,” 2024. [Online]. Available: <https://arxiv.org/abs/2409.12416>
- [27] V. Sechaud, L. Jacques, P. Abry, and J. Tachella, “Equivariance-based self-supervised learning for audio signal recovery from clipped measurements,” 2024. [Online]. Available: <https://arxiv.org/abs/2409.15283>
- [28] M. Švento, P. Rajmic, and O. Mokry, “Plug-and-play audio restoration with diffusion denoiser,” in *2024 18th International Workshop on Acoustic Signal Enhancement (IWAENC)*, vol. 1. IEEE, Sep. 2024, pp. 115–119. [Online]. Available: <https://ieeexplore.ieee.org/document/10694642>
- [29] A. van den Oord, S. Dieleman, H. Zen, K. Simonyan, O. Vinyals, A. Graves, N. Kalchbrenner, A. Senior, and K. Kavukcuoglu, “WaveNet: A generative model for raw audio,” in *Proc. 9th ISCA Workshop on Speech Synthesis Workshop (SSW 9)*, 2016.
- [30] O. Triebe, N. Laptev, and R. Rajagopal, “Ar-net: A simple autoregressive neural network for time-series,” 2019. [Online]. Available: <https://arxiv.org/abs/1911.12436>
- [31] P. J. Brockwell and R. A. Davis, *Time Series: Theory and Methods*, 2nd ed., ser. Springer series in statistics. Springer, 2006.
- [32] J. Durbin, “The fitting of time-series models,” *Revue de l’Institut International de Statistique / Review of the International Statistical Institute*, vol. 28, no. 3, p. 233, 1960.
- [33] N. Levinson, “The Wiener (root mean square) error criterion in filter design and prediction,” *Journal of Mathematics and Physics*, vol. 25, no. 1-4, pp. 261–278, Apr. 1946.
- [34] M. Aharon, M. Elad, and A. M. Bruckstein, “K-SVD: An algorithm for designing of overcomplete dictionaries for sparse representations,” *IEEE Transactions on Signal Processing*, vol. 54, pp. 4311–4322, 2006.
- [35] J. Gorski, F. Pfeuffer, and K. Klamroth, “Biconvex sets and optimization with biconvex functions: a survey and extensions,” *Mathematical Methods of Operations Research*, vol. 66, no. 3, pp. 373–407, Jun. 2007.
- [36] S. P. Boyd, N. Parikh, E. Chu, B. Peleato, and J. Eckstein, “Distributed optimization and statistical learning via the alternating direction method of multipliers,” *Foundations and Trends in Machine Learning*, vol. 3, no. 1, pp. 1–122, 2011. [Online]. Available: <http://dblp.uni-trier.de/db/journals/ftml/ftml3.html#BoydPCPE11>
- [37] P. Combettes and J. Pesquet, “Proximal splitting methods in signal processing,” *Fixed-Point Algorithms for Inverse Problems in Science and Engineering*, vol. 49, pp. 185–212, 2011.
- [38] A. Beck, *First-Order Methods in Optimization*. SIAM-Society for Industrial and Applied Mathematics, 2017.
- [39] I. Bayram, “Proximal mappings involving almost structured matrices,” *IEEE Signal Processing Letters*, vol. 22, no. 12, pp. 2264–2268, Dec. 2015.
- [40] A. Adler, V. Emiya, M. G. Jafari, M. Elad, R. Gribonval, and M. D. Plumbley, “Audio Inpainting,” *IEEE Transactions on Audio, Speech, and Language Processing*, vol. 20, no. 3, pp. 922–932, Mar. 2012.
- [41] R. Huber and B. Kollmeier, “PEMO-Q—A new method for objective audio quality assessment using a model of auditory perception,” *IEEE Trans. Audio Speech Language Proc.*, vol. 14, no. 6, pp. 1902–1911, Nov. 2006.
- [42] T. Thiede, W. C. Treurniet, R. Bitto, C. Schmidmer, T. Sporer, J. G. Beerends, C. Colomes, M. Keyhl, G. Stoll, K. Brandenburg, and B. Feiten, “PEAQ – The ITU standard for objective measurement of perceived audio quality,” *Journal of the Audio Engineering Society*, vol. 48, no. 1/2, pp. 3–29, January/February 2000. [Online]. Available: <http://www.aes.org/e-lib/browse.cfm?elib=12078>
- [43] P. Kabal, “An examination and interpretation of ITU-R BS.1387: Perceptual evaluation of audio quality,” MMSP Lab Technical Report, Dept. Electrical & Computer Engineering, McGill University, Tech. Rep., May 2002.
- [44] (2008) EBU SQAM CD: Sound quality assessment material recordings for subjective tests. online. [Online]. Available: <https://tech.ebu.ch/publications/sqamcd>



Ondřej Mokří started to work on optimization methods for restoration of corrupted audio signals under the guidance of Pavel Rajmic during his bachelor and master studies. He further developed this topic in his doctoral studies at the Faculty of Electrical Engineering and Communication, Brno University of Technology, which he successfully completed in 2024. In addition to sparse and structured signal representations, he is interested in combining classical optimization methods with deep learning.



Pavel Rajmic finished his Ph.D. studies in signal processing in 2004 and since then he has been employed at the Faculty of Electrical Engineering and Communication, Brno University of Technology. As a member of the SPLab team, his interests include signal processing, applied and computational mathematics, frame theory and applications, sparse signal modeling, and compressed sensing.